Title
Fermentation of hydrolysate detoxified by pervaporation through block copolymer membranes

Journal
Green Chemistry, 16(9)

ISSN
1463-9262

Authors
Greer, Douglas R
Basso, Thalita P
Ibanez, Ana B
et al.

Publication Date
2014

DOI
10.1039/c4gc00756e

Peer reviewed

Green Chemistry

PAPER

View Article Online
View Journal | View Issue

CrossMark click for updates

Cite this: *Green Chem.*, 2014, **16**, 4206

Fermentation of hydrolysate detoxified by pervaporation through block copolymer membranes†

Douglas R. Greer,[a] Thalita P. Basso,[b] Ana B. Ibanez,[c] Stefan Bauer,[c] Jeffrey M. Skerker,[b] A. Evren Ozcam,[a] Dacia Leon,[c] Chaeyoung Shin,[a] Adam P. Arkin*[b] and Nitash P. Balsara*[a,d,e]

Received 28th April 2014,
Accepted 24th June 2014

DOI: 10.1039/c4gc00756e

www.rsc.org/greenchem

The large-scale use of lignocellulosic hydrolysate as a fermentation broth has been impeded due to its high concentration of organic inhibitors to fermentation. In this study, pervaporation with polystyrene-block-polydimethylsiloxane-block-polystyrene (SDS) block copolymer membranes was shown to be an effective method for separating volatile inhibitors from dilute acid pretreated hydrolysate, thus detoxifying hydrolysate for subsequent fermentation. We report the separation of inhibitors from hydrolysate thermodynamically and quantitatively by detailing their concentrations in the hydrolysate before and after detoxification by pervaporation. Specifically, we report >99% removal of furfural and 27% removal of acetic acid with this method. Additionally, we quantitatively report that the membrane is selective for organic inhibitor compounds over water, despite water's smaller molecular size. Because its inhibitors were removed but its sugars left intact, pervaporation-detoxified hydrolysate was suitable for fermentation. In our fermentation experiments, *Saccharomyces cerevisiae* strain SA-1 consumed the glucose in pervaporation-detoxified hydrolysate, producing ethanol. In contrast, under the same conditions, a control hydrolysate was unsuitable for fermentation; no ethanol was produced and no glucose was consumed. This work demonstrates progress toward economical lignocellulosic hydrolysate fermentation.

1. Introduction

Lignocellulosic feedstocks are a potential large-scale source of renewable energy, transportation fuel, and organic chemicals.[1] As lignocellulosic biomass is the most abundantly available source of biomass, its feedstocks are a prospect to replace fossil fuels as a source of chemicals and energy.[2] Many plant species can be used as lignocellulosic feedstocks, but for the purpose of this study, we choose *Miscanthus* × *giganteus*, a plant species in focus of research at our institute. *Miscanthus* × *giganteus* is a tall perennial grass hybrid bred for its extraordinary capacity to fix carbon. When compared to corn, *Miscanthus* produces more biomass per acre, requires less fertilization and water input, lives through the year, and does not compete as a food crop.[3,4]

Lignocellulosic feedstocks are typically processed in two steps: first, cellulose and hemicellulose are depolymerized to soluble sugars. Second, these sugars are converted by fermentation into high value products such as alcohols.[5] In this study, common methods for pretreatment and fermentation are used: partial depolymerization of *Miscanthus* is achieved with heat and dilute acid pretreatment, and yeast is used to produce ethanol by fermentation.[6,7] The product of the depolymerization step is called hydrolysate. Unfortunately, the depolymerization step also produces toxic inhibitors such as acids, furans, and phenols.[8,9] These inhibitors, through a number of biological mechanisms both known and unknown,[10,11] reduce the overall ethanol yield, retard ethanol production, and even prevent fermentation.[12] In fact, the inhibitors exhibit such acute toxicity that additional detoxification steps are required.[9] Techniques for detoxification of lignocellulosic hydrolysates include but are not limited to alkali[13] or other chemical addition,[14] enzymatic treatment,[15] liquid–liquid extraction,[16] sorption,[17] and ion exchange.[18] However, commonly studied detoxification methods typically require additional inputs or

[a]*Department of Chemical and Biomolecular Engineering, University of California, Berkeley, California 94720, USA. E-mail: nbalsara@berkeley.edu; Tel: +1 (510) 642-8937*
[b]*Department of Bioengineering, University of California, Berkeley, California 94720, USA. E-mail: aparkin@lbl.gov; Tel: +1 (510) 643-5678*
[c]*Energy Biosciences Institute, University of California, Berkeley, California 94704, USA*
[d]*Materials Sciences Division, Lawrence Berkeley National Laboratory, Berkeley, California 94720, USA*
[e]*Environmental Energy Technologies Division, Lawrence Berkeley National Laboratory, Berkeley, California 94720, USA*
†Electronic supplementary information (ESI) available. See DOI: 10.1039/c4gc00756e

separation processes, for example, using inorganic lime for detoxification requires the additional separation of a highly alkaline solid phase.[19,20]

In this study, we explored the feasibility of pervaporation as a means to remove inhibitors. Pervaporation is the combination of two words, permeation and evaporation. These two combined phenomena can be accomplished using a polymer membrane. With dense membranes, *i.e.* non-porous membranes, the pervaporated species sorb onto the membrane surface, diffuse across the membrane, and evaporate into an evacuated vessel maintained at low pressure. Pervaporation is driven by gradients in chemical potentials. Volatile species are thermodynamically favored to evaporate into the evacuated vessel, and these species are pervaporated at different rates due to differences in sorption equilibria and diffusion kinetics.[21] The starting material is called the feed, the pervaporated material is called the permeate, and the remaining non-pervaporated material is called the retentate. Membrane pervaporation has the potential to reduce the energy required for biofuel purification and to increase the efficiency of biofuel production.[22]

Previously, pervaporation has been studied as a method for the separation of water and furfural for green chemistry applications.[23] Pervaporation has also been used as part of a joint hydrolysate detoxification process in which pervaporation removed furfural, and the enzyme laccase removed phenolic compounds, a process which ultimately improved fermentation.[24] However, this is the first work wherein pervaporation is used as the sole hydrolysate detoxification method and in-depth quantification of inhibitor removal, thermodynamic driving force analysis, and subsequent fermentation analysis are detailed.

We performed pervaporation on a *Miscanthus* hydrolysate using a microphase separated polystyrene-block-polydimethylsiloxane-block-polystyrene (SDS) copolymer membrane. Microphase separation forms co-continuous polystyrene (PS) and polydimethylsiloxane (PDMS) domains. Our objective was to remove the inhibitors from hydrolysate by pervaporation while leaving fermentable sugars intact. The PDMS domains have good transport properties for organic species as PDMS is a good transporter of ethanol and other organic compounds.[25] The PS domains are rigid and provide the membrane with structural integrity. SDS copolymer membranes are more selective for organic compounds relative to commercially available cross-linked PDMS membranes.[26] The efficacy of the pervaporation-based process was demonstrated by fermentation, using the pervaporation-detoxified hydrolysate and *Saccharomyces cerevisiae* strain SA-1, a robust strain isolated in 1993 from a Brazilian Copersucar industrial plant which produced bioethanol from sugarcane substrates.[27]

2. Experimental

Membrane properties and testing

Polymer Source (Montreal) provided the SDS copolymer, which was used as received. The product was labeled with the following properties: number averaged molecular weight of the middle PDMS block was 104 kg mol^{-1}, number averaged molecular weight of each end PS block was 22 kg mol^{-1}, polydispersity index of the copolymer was 1.3, and 86 weight% of the sample was the triblock copolymer (the remainder was mainly the diblock copolymer).

In 20 mL cyclohexane (Sigma Aldrich, used as received), 1 g SDS was stirred and dissolved. This solution was spin casted on a Biomax 50 PBQK 20 cm × 20 cm nanofiltration support membrane, and cut to fit our pervaporation cells. The pervaporation membrane was formed by casting three separate aliquots of 7 mL solution at 1300 rpm onto the support with 1 min for drying between aliquot applications. The membrane was then placed in a vacuum oven at room temperature to remove excess solvent. The average thickness for SDS membranes formed by this method was 10 μm.

The pervaporation flux of deionized water through the membranes thus obtained was measured at 70 °C and compared with that obtained using an unsupported SDS membrane of 120 μm micrometer-measured thickness. The thicknesses of the two supported membranes used in this study were determined to be 8 and 12 μm from these measurements by assuming that water permeability is independent of membrane thickness (see eqn (1)). The fluxes were 4.7 and 3.1 g h^{-1} for the 8 and 12 μm thick membranes.

Dilute acid hydrolysis

Hydrolysate was obtained from the National Renewable Energy Lab (NREL) with the following conditions: *Miscanthus × giganteus* plant material (around 1 inch size) was pretreated with 1.5% (w/w) sulfuric acid at a 25% (w/w) biomass loading at 190 °C for approximately 1 minute, and then the pressure was rapidly released. The liquid phase after filtration is referred to as hydrolysate. In some industrial processes, hydrolysate is subjected to enzymatic hydrolysis. In this study, the hydrolysate was used as received. Upon receipt, the hydrolysate thus obtained was stored at −20 °C. Before pervaporation, the hydrolysate was thawed, centrifuged at 2000*g* for 10 min, filtered through a Whatman 2 V folded filter paper, and its pH was increased to 3.0 by adding KOH. The resulting hydrolysate contained a complex mixture of inhibitory organic compounds (see ESI Table AI†).

Pervaporation

Pervaporation of hydrolysate was performed in a laboratory bench test unit built by Sulzer Chemtech, Germany and described previously.[28] The two membranes were used in parallel, contributing a permeation area of 37 cm^2 apiece. The SDS membranes were held inside a circular cell restrained with an O-ring. The temperature of the feed was controlled in the range of 70 ± 1 °C. The experiment began with 530 mL of hydrolysate in the feed tank. A vacuum of <3 mbar was applied using a vacuum pump on the permeate side of the membranes (Welch, model 2014). Permeates were condensed in a cold trap (ChemGlass CG-4516-02) cooled with liquid nitrogen. Permeate samples were weighed to determine the mass permeated

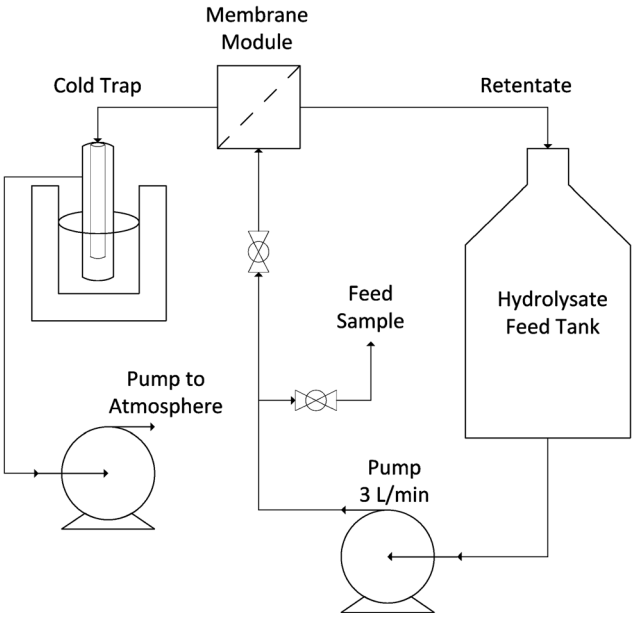

Fig. 1 Schematic diagram of the pervaporation apparatus. Hydrolysate was pumped across a membrane module and the retentate was returned to the feed tank and mixed. The permeated species was collected in a cold trap under vacuum.

through the membrane during the experiment. The hydrolysate retentate retained in the feed tank after 24 h of pervaporation was used in the fermentation experiments described below and was called pervaporation-detoxified hydrolysate. The SDS membranes were then replaced by impermeable nonporous Teflon membranes. A control hydrolysate sample was prepared starting with a fresh feed of 530 mL of pH 3 hydrolysate in the feed tank and pumping it through the pervaporation apparatus for 24 h at 70 °C. No pervaporation occurred in this control experiment.

Fig. 1 depicts the schematic of the pervaporation apparatus. In pervaporation and control experiments, feed samples were collected approximately every 90 minutes. In the pervaporation experiment, samples were also collected from the permeate cold trap.

Glucose, xylose, acetate, ethanol, 5-hydroxyfurfural, and furfural were analyzed using the high pressure liquid chromatography (HPLC) method[29] on a system (Agilent Technologies, Santa Clara, CA, USA) equipped with a refractive index detector (RID). Samples were injected onto a 300 mm × 7.8 mm Aminex HPX-87H column (BioRad, Richmond, CA, USA) with a guard column of the same material. Elution was performed at 50 °C with 5 mM sulfuric acid at a flow rate of 0.6 mL min^{-1}. We chose glucose as the normalization standard because it has a high concentration and does not degrade under experimental conditions, as observed in our repeated preliminary studies. In *Miscanthus* hydrolysate, galactose and mannose are also present, but in lower concentration. These sugars co-elute with xylose on the HPLC column used and therefore the three sugars were quantified together as "xylose".

Gas chromatography and mass spectroscopy (GCMS) analysis of the compounds was performed as described previously.[30] Briefly, 1 mL of hydrolysate was spiked with the internal standard 4-isopropylphenol and the mixture extracted four times, each with 0.5 mL of ethyl acetate. The ethyl acetate phases were combined, mixed and dried over sodium sulfate. An aliquot was derivatized with *N*,*O*-bis(trimethylsilyl)-trifluoroacetamide (BSTFA) containing 1% trimethylchlorosilane (TMCS). 1 μL was injected in splitless mode onto a VF5-ms capillary column (30 m × 0.25 mm × 0.25 μm, Agilent, Santa Clara). An Agilent 7890A gas chromatograph coupled to an Agilent 5975C single quadrupole mass spectrometer was used for analysis.

Organic acids were quantified using liquid chromatography and mass spectroscopy (LCMS) (QTOF, Agilent Technologies, Santa Clara, CA, USA) in negative ion mode.

Thermodynamic properties calculation

The molar flux of pervaporated species i, J_i, is given by Wijmans and Baker,[21]

$$J_i = \frac{P_i}{t}(x_i\gamma_i p_i^{\mathrm{sat}} - y_i p_{\mathrm{p}})[=]\frac{\mathrm{mol}}{\mathrm{m^2 s}}, \quad (1)$$

where P_i is the permeability of the membrane, t is the membrane thickness (SDS copolymer only), x_i is the feed mole fraction, γ_i is the activity coefficient, p_i^{sat} is the saturated vapor pressure, y_i is the permeate mole fraction and p_{p} is the total permeate pressure. In our experiments we approximated the product $y_i p_{\mathrm{p}}$ to zero because of the low permeate pressure (<3 mbar). In our experiments, the water permeability was calculated to be 5.1×10^{-12} mol m m^{-2} Pa s.

The separation factor for pervaporation, β_{pervap}, is a measure of the enrichment of species i compared to another species, in our case, water.

$$\beta_{\mathrm{pervap}} = \frac{c_{i\mathrm{p}}/c_{\mathrm{wp}}}{c_{i\mathrm{h}}/c_{\mathrm{wh}}}, \quad (2)$$

where c denotes concentration (g L^{-1}), subscript w denotes water, subscript p denotes permeate, and subscript h denotes hydrolysate feed. *E.g.* $c_{i\mathrm{p}}$ denotes the concentration of species i found in the permeate, detected by HPLC, LCMS, or GCMS.

The separation factor for evaporation, β_{evap}, is a measure of the enrichment of species i compared to water due to evaporation alone.

$$\beta_{\mathrm{evap}} = \frac{p_i/p_{\mathrm{w}}}{x_i/x_{\mathrm{w}}} = \frac{\gamma_i p_i^{\mathrm{sat}} u_i}{p_{\mathrm{w}}^{\mathrm{sat}}}, \quad (3)$$

where p_i is the pressure of component i in the gas phase and p_{w} is the pressure of water in the gas phase. Aqueous binary activity coefficients, γ_i, were obtained from Gmehling *et al.*,[31] and the fraction of undissociated acid molecules, u_i, was obtained from Green and Perry,[32] *i.e.*, $HA \leftrightarrow H^+ + A^-$; $u_i = [HA]/([HA] + \lfloor A^- \rfloor)$. Ideally, multicomponent thermodynamic parameters should be used to model a multicomponent vapor–liquid equilibrium. However, there is little multicomponent

thermodynamic data in the literature. Because the hydrolysate solution contains more than 90% water, we expect water–water and water–solute interactions to dominate. We thus expect the binary thermodynamics to provide a reasonable starting point for modeling the vapor–liquid equilibrium of hydrolysate.

The membrane selectivity, α_{mem}, is a measure of the enrichment of species i compared to water due to permeation through the membrane alone.

$$\alpha_{mem} = \frac{P_i}{P_w} = \frac{\beta_{pervap}}{\beta_{evap}} = \frac{p_w^{sat}}{\gamma_i p_i^{sat} u_i} \times \frac{c_{ip}/c_{wp}}{c_{ih}/c_{wh}}, \quad (4)$$

where P_w is the permeability of water. Implicit in this analysis is the assumption that the binary aqueous parameters γ_i and u_i are applicable in our multicomponent hydrolysate system.

Yeast culture and fermentation

The yeast strain *Saccharomyces cerevisiae* SA-1 was provided by the Yeast Biochemistry and Technology Laboratory, Biological Science Department, Luiz de Queiroz College of Agriculture, University of Sao Paulo, Brazil. Stock cultures were grown at 30 °C for 3 days in YPD medium (10 g L^{-1} yeast extract, 20 g L^{-1} peptone, 20 g L^{-1} glucose) supplemented with 20 g L^{-1} agar for solid culture. Two biologically duplicate colonies were grown at 30 °C at 200 rpm in an Innova 2000 platform shaker overnight using 10 mL of synthetic complete media (SC-80). SC-80 contains 80 g L^{-1} glucose, 2 g L^{-1} dropout mix (US Biological), 6.7 g L^{-1} yeast nitrogen base (Becton, Dickinson and Company), 19.5 g L^{-1} MES buffer, and a small amount of KOH to adjust the pH to 5.5. After overnight growth, cells were harvested by centrifugation.

Fermentation was performed in 25 mL Hungate bottles under anaerobic conditions. The pervaporation-detoxified hydrolysate fermentation broth contained pervaporation-detoxified hydrolysate, water to match the amount removed by pervaporation, and harvested yeast cells, and had an initial OD600 of 0.3. The control hydrolysate fermentation broth contained control hydrolysate and harvested yeast cells, and had an initial OD600 of 0.3. The OD600 of values of 0.3 included background subtraction to account for hydrolysate absorption. The fermentation was performed at 34 °C and 200 rpm using a Certomat BS-1 Sartorius shaker for time = 0–50 h and room temperature with no shaking for time = 50–312 h. Additionally, control and pervaporation-detoxified hydrolysate fermentations were performed under these same conditions at 34 °C and 200 rpm for time = 0–119.5 h, with the addition of the components of SC-80 to match SC-80 levels.

During fermentation, OD600, ethanol concentration, and glucose concentration were measured under aseptic conditions. 50 μL of fermentation broth were used to measure the OD600 using a Genesys 20 Visible Spectrophotometer. Simultaneously, 250 μL were centrifuged, filtered, and analyzed for glucose and ethanol concentrations using the HPLC system described above.

3. Results and discussion

Hydrolysate is a complex mixture comprising a multitude of organic compounds. Our HPLC, GCMS, and LCMS methods detect around 100 compounds thereof. The concentrations of these compounds in the hydrolysate before and after pervaporation are given in the ESI Table AI.† The end alcohol content of the subsequent fermentation depends on its starting sugar concentration. The three sugars quantified in our hydrolysate are glucose, xylose, and arabinose. The short list of our focus inhibitors in hydrolysate is acetic acid, formic acid, furfural, and guaiacol. This short list contains at least one member of each of the main inhibitor classes: acids, furans, and phenolics. Our objective is to use pervaporation to remove the inhibitors without affecting the sugar and then determine the biological consequences of detoxification by fermentation using the *Saccharomyces cerevisiae* strain SA-1.

The effect of our 70 °C 24 h pervaporation treatment on hydrolysate is summarized in Fig. 2 and Table 1. The abscissa in Fig. 2 gives the initial concentrations of the compounds of interest. The blue bars display the mass percent of these compounds removed by pervaporation. Also shown in Fig. 2

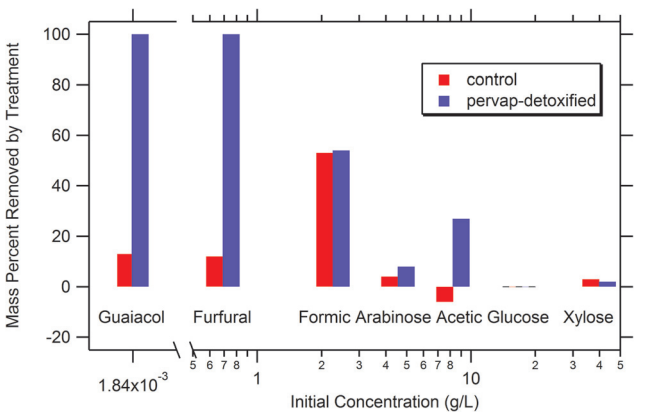

Fig. 2 Measured removal of inhibitors and sugars by treatment *versus* their initial concentration. Results of pervaporation treatment are shown with blue bars and results of control treatment are shown with red bars. Glucose is used as an internal standard and its removal is zero by definition. A pervaporation detoxification significantly removes inhibitors without the removal of sugars.

Table 1 Starting concentrations of select compounds in hydrolysate and their mass% retained in the hydrolysate after 24 hours of pervaporation or control treatment

Species	c_{ihi} (g L^{-1})	Mass% pervap	Mass% control
Xylose	45	98	97
Glucose	19	100	100
Acetic acid	8.7	73	106
Arabinose	5.1	92	96
Formic acid	2.5	47	46
Furfural	0.80	0	88
Guaiacol	0.0018	0	87

c_{ihi} is the species i concentration initially in the hydrolysate feed. Glucose is used as an internal standard.

are changes in the concentration of the compounds of interest due to heat treatment alone, as determined in our control experiment, wherein the hydrolysate is heated to 70 °C and pumped through the system for 24 h. These results are represented by the red bars in Fig. 2. The change in glucose concentration is identically zero, because we use this component as an internal standard for our concentration determinations. Slight decreases in the normalized masses of xylose (2%) and arabinose (8%) are seen during pervaporation (Fig. 2). Similar decreases are seen in the control experiment. We attribute the observed consumption of sugars to reactions that occur spontaneously in hydrolysate at 70 °C. To a good approximation, the pervaporation process leaves the sugars intact.

It is evident in Fig. 2 that guaiacol and furfural, both uncharged inhibitors, are efficiently removed by pervaporation. After pervaporation-detoxification, the concentrations of these species in the hydrolysate are not detected. About 10% of guaiacol and furfural are consumed in the control experiment, indicating that some of the removal of these species during experimentation is attributable to chemical reactions. The amount of formic acid removed in the control and pervaporation experiments are similar. This suggests that pervaporation has a limited effect on formic acid. The concentration of acetic acid increases slightly in the control experiment. The observed 27% removal of acetic acid by pervaporation treatment (Fig. 2) is attributed to permeation and evaporation across the membrane.

Table 2 shows the concentrations of the inhibitors in the hydrolysate and the permeate at the beginning of pervaporation (time = 0–2 h) and end of pervaporation (time = 22–24 h). The water concentration in the hydrolysate ($c_{i\mathrm{h}}$) decreases as pervaporation proceeds, starting at 945 g L^{-1} and ending at 906 g L^{-1}. The water concentration in the permeate ($c_{i\mathrm{p}}$) increases as pervaporation proceeds, starting at 985 g L^{-1} and ending at 991 g L^{-1}. The reason for this will be made clear shortly. The main inhibitor removed by pervaporation is furfural. Pervaporation of hydrolysate containing 0.69 g L^{-1} of furfural results in an aqueous permeate with 6.3 g L^{-1} of furfural. From these measurements, the calculated pervaporation separation factor, β_{pervap}, of furfural in our SDS membrane is 8.6. This is consistent with the published literature on furfural pervaporation. Guaiacol is also effectively removed by pervaporation, β_{pervap} = 11. Acetic acid is found in the hydrolysate and permeate in the beginning and the end of pervaporation. The pervaporation separation factors obtained in the beginning and at the end are similar (0.77 and 0.73). Our β_{pervap} data for guaiacol, furfural, and acetic acid are similar to those found in the previous literature.[23,33] Formic acid is found in permeate at the end of pervaporation with a relatively low pervaporation separation factor, β_{pervap} = 0.11. By the end of the pervaporation (time = 22–24 h), furfural and guaiacol have completely permeated and are neither found in the permeate nor in the hydrolysate samples taken at this time point. The concentration of water in the final permeate sample (time t = 22–24 h) is higher because it contains no furfural (the hydrolysate also contains no furfural).

The vapor–liquid equilibrium data of the compounds of interest listed in Table 2 enable determination of the driving forces and membrane properties of the separations described above. The separation factors due to evaporation alone, β_{evap}, are listed in Table 2 (we were unable to obtain γ_i for guaiacol). It is perhaps worth noting that evaporation of furfural is driven by its large activity coefficient (γ_i = 85); the saturation pressure of furfural relative to that of water is only 0.096. The membrane selectivity factors for acetic acid and furfural are in the vicinity of 1.1. These membrane selectivity values are remarkably similar to values reported for ethanol transport through SDS membranes.[26] Upon first impression, membrane selectivity values of approximately 1.1 may seem unremarkable. However, because water has a much smaller molecular size than furfural or ethanol, pervaporation membranes selective for organic species must overcome the quicker diffusion associated with smaller molecules. In addition to PDMS, important examples of the chemistry of organic-selective polymer membranes include poly[1-(trimethylsilyl)-1-propyne] (PTMSP), and polymers of intrinsic microporosity (PIMs) such as PIM-1 and PIM-7.[34]

Fermentation experiments were performed on pervaporation-detoxified and control hydrolysates. The results are shown in Fig. 3. The pH of the hydrolysates was adjusted to 5.5 using KOH. Because water is permeated during pervaporation, water was added to the pervaporation sample until the glucose levels in the pervaporation sample and control sample were matched. *Saccharomyces cerevisiae* SA-1 cells were added to the treated hydrolysate samples at time = 0. The concentrations of

Table 2 Toxin removal by pervaporation: pervaporation separation data, vapor–liquid equilibrium properties, and membrane selectivity

	Pervaporation data			Vapor–liquid equilibrium data				Membrane properties	
	$c_{i\mathrm{h}}$ (g L^{-1})	$c_{i\mathrm{p}}$ (g L^{-1})	β_{pervap}	$p_i^{\mathrm{sat}}/p_{\mathrm{w}}^{\mathrm{sat}\,a}$	γ_i	u_i	β_{evap}	α_{memb}	P_i (mol m m^{-2} Pa^{-1} s^{-1})
Water[b]	906	991	1	1	1	1	1	1	5.1×10^{-12}
Water[c]	945	985	1	1	1	1	1	1	5.1×10^{-12}
Acetic acid[b]	10	8.6	0.77	0.57	1.17	0.99	0.67	1.15	5.9×10^{-12}
Acetic acid [c]	8.2	6.3	0.73	0.57	1.17	0.99	0.67	1.09	5.6×10^{-12}
Formic acid[c]	1.7	0.22	0.11	1.2	0.35	0.86	0.36	0.31	1.6×10^{-12}
Furfural[c]	0.69	6.3	8.6	0.096	85	1	8.2	1.05	5.4×10^{-12}
Guaiacol[c]	0.0016	0.17	11	0.1	—	1	—	—	—

[a] The absolute vapor pressure of water, $p_{\mathrm{w}}^{\mathrm{sat}}$, at 70° C is 31 086 Pa. [b] Concentration values measured at the end of pervaporation (t = 22 to t = 24 h). [c] Concentration values measured at the beginning of pervaporation (t = 0 to t = 2 h). See eqn (1)–(4) for parameter definitions and relationships. All parameters at 70 °C and hydrolysate pH 3.0.

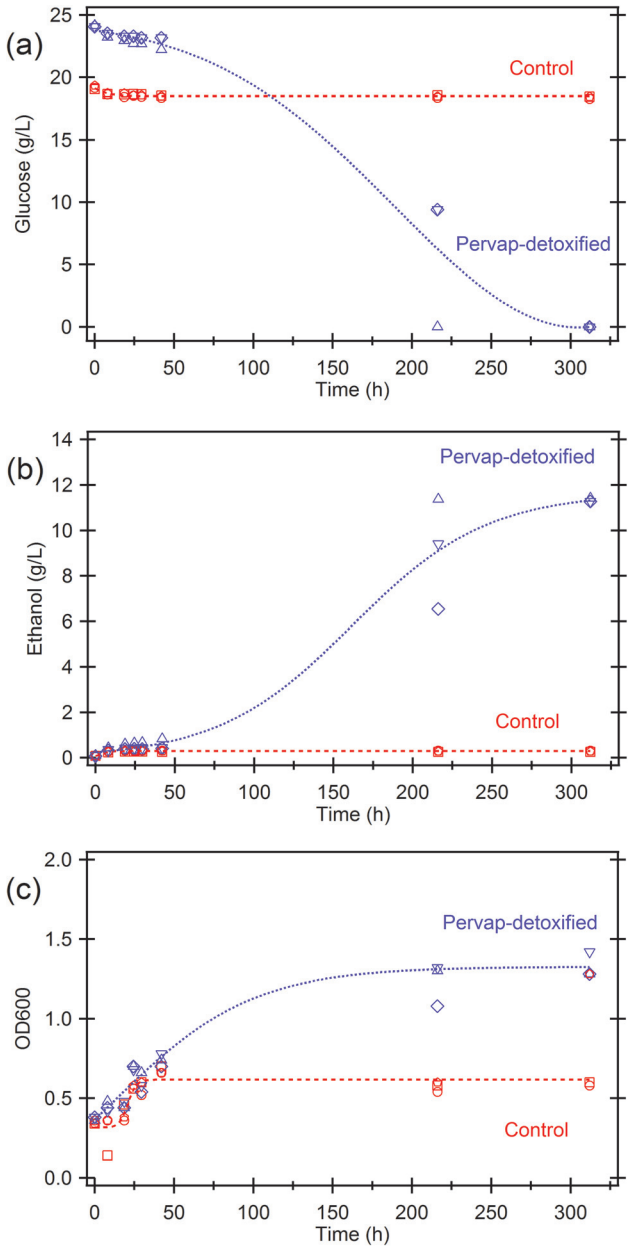

Fig. 3 Fermentation data of the pervaporation-detoxified hydrolysate and control hydrolysate *versus* time are shown. (a) Glucose and (b) ethanol concentrations were measured by HPLC and (c) optical density was measured at 600 nm (OD600). (a–c) The data from three fermentation experiments are shown with curves to guide the eye.

glucose and ethanol were monitored for 312 h and the results are shown in Fig. 3a and b. (The small difference in initial glucose concentration is due to the water added with the aqueous cell cultures.) In the case of pervaporation-detoxified hydrolysate, both Fig. 3a and b show evidence for slow conversion of glucose into ethanol. In contrast, the change in glucose (Fig. 3a) and ethanol (Fig. 3b) concentrations in the control hydrolysate over time = 0–312 h are negligible. The time dependence of OD600 is shown in Fig. 3c. In the pervaporation-detoxified hydrolysate we see an increase in OD600 (Fig. 3c) accompanying ethanol production (Fig. 3b). In the control hydrolysate, OD600 approximately doubled in the first 50 h, which we attribute to one cellular division. However, the inhibitors in the control hydrolysate interfere with yeast growth processes. There was no sustained growth (Fig. 3c) in the control hydrolysate and thus no consumption of glucose (Fig. 3a) or production of ethanol (Fig. 3b). The data show that pervaporation-detoxified hydrolysate is suitable for fermentation and ethanol production. All the glucose is consumed, and converted primarily into ethanol. To our knowledge, this is the

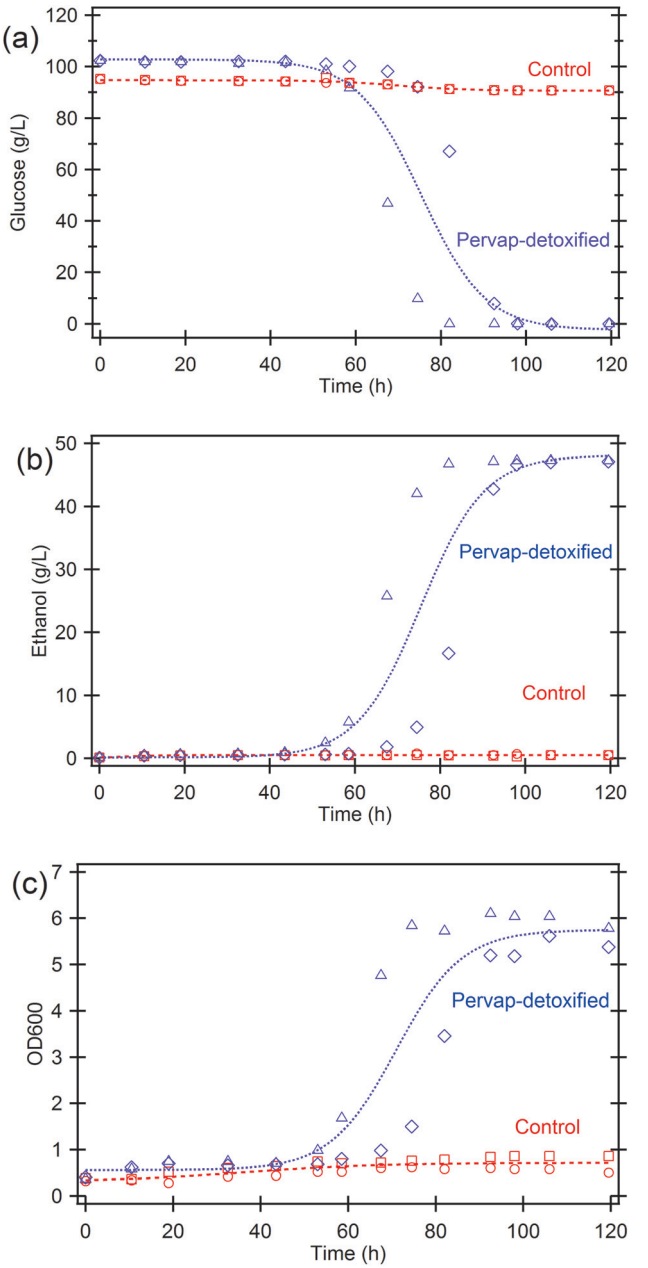

Fig. 4 SC-80 nutrients are added to Pervaporation-detoxified hydrolysate and control hydrolysate and these mixtures are fermented. In the fermentation broths, (a) glucose concentration, (b) ethanol concentration, and (c) optical density at 600 nm (OD600) were measured and are plotted *versus* time. (a–c) The data from two fermentation experiments are shown with curves to guide the eye.

first experiment demonstrating that the detoxification of pretreated hydrolysate by pervaporation alone is sufficient for ethanol production by fermentation with yeast.

An additional set of fermentation experiments were performed on pervaporation-detoxified and control hydrolysates, as shown in Fig. 4. In this fermentation, SC-80 nutrient components were added before fermentation. This was done because *Saccharomyces cerevisiae* SA-1 cells flourish in SC-80 nutrient. Again, the pH of the hydrolysates were adjusted to 5.5 using KOH, water was added to the pervaporation sample until the glucose levels in the pervaporation sample and control sample were matched, and *Saccharomyces cerevisiae* SA-1 cells were added to the treated hydrolysate samples at time = 0. The concentrations of glucose and ethanol were monitored for 119.5 h and the results are shown in Fig. 4a and b. Pervaporation-treated hydrolysate fermentation shows glucose (Fig. 4a) conversion into ethanol (Fig. 4b). In contrast, the change in glucose (Fig. 4a) and ethanol (Fig. 4b) concentrations in the control hydrolysate over time = 0–119.5 h is negligible. In the pervaporation-detoxified hydrolysate, a steady increase in OD600 (Fig. 4c) accompanies ethanol production (Fig. 4b). The data demonstrate that pervaporation-detoxified hydrolysate is suitable for ethanol production by fermentation. With the addition of SC-80 components to the pervaporation-detoxified hydrolysate, fermentation proceeds quicker and produces more ethanol. Despite the wealth of nutrients provided by the SC-80 components, the inhibitors in the control hydrolysate prevent its fermentation.

4. Conclusion

In this study, pervaporation with a polystyrene-block-polydimethylsiloxane-block-polystyrene membrane has demonstrated the ability to remove inhibitors from *Miscanthus* × *giganteus* dilute acid pretreated lignocellulosic hydrolysate, while leaving sugars intact. The thermodynamics for separation are elucidated, showing the membrane's selectivity for furfural and acetic acid over water. Our in-depth thermodynamic analysis allows for future calculations and comparison of hydrolysate separation techniques. Furthermore, the pervaporation-treated hydrolysates are suitable for ethanol fermentation with *Saccharomyces cerevisiae* strain SA-1 with and without further nutrient addition. These results indicate that pervaporation is a viable approach for hydrolysate detoxification in an industrial bioethanol production process.

Competing Interest

The authors declare no competing financial interest.

Acknowledgements

This work was funded by the Energy Biosciences Institute. Hydrolysate was provided by the National Renewable Energy Laboratory, 1617 Cole Blvd., Golden, CO 80401, a national laboratory of the U.S. Department of Energy managed by the Alliance for Sustainable Energy, LLC for the U.S. Department of Energy under Contract Number DE-AC36-08GO28308.

Notes and references

1 A. Carroll and C. Somerville, *Annu. Rev. Plant Biol.*, 2009, **60**, 165–182.
2 M. E. Himmel, S.-Y. Ding, D. K. Johnson, W. S. Adney, M. R. Nimlos, J. W. Brady and T. D. Foust, *Science*, 2007, **315**, 804–807.
3 J. C. Clifton-Brown, J. Breuer and M. B. Jones, *Glob. Chang. Biol.*, 2007, **13**, 2296–2307.
4 I. Lewandowski, J. C. Clifton-Brown, J. M. O. Scurlock and W. Huisman, *Biomass Bioenergy*, 2000, **19**, 209–227.
5 E. M. Rubin, *Nature*, 2008, **454**, 841–845.
6 N. Mosier, C. Wyman, B. Dale, R. Elander, Y. Y. Lee, M. Holtzapple and M. Ladisch, *Bioresour. Technol.*, 2005, **96**, 673–686.
7 C. C. Geddes, I. U. Nieves and L. O. Ingram, *Curr. Opin. Biotechnol.*, 2011, **22**, 312–319.
8 S. Bauer, H. Sorek, V. D. Mitchell, A. B. Ibáñez and D. E. Wemmer, *J. Agric. Food Chem.*, 2012, **60**, 8203–8212.
9 H. B. Klinke, A. B. Thomsen and B. K. Ahring, *Appl. Microbiol. Biotechnol.*, 2004, **66**, 10–26.
10 J. M. Skerker, D. Leon, M. N. Price, J. S. Mar, D. R. Tarjan, K. M. Wetmore, A. M. Deutschbauer, J. K. Baumohl, S. Bauer, A. B. Ibáñez, V. D. Mitchell, C. H. Wu, P. Hu, T. Hazen and A. P. Arkin, *Mol. Syst. Biol.*, 2013, **9**, 674.
11 T. A. Clark and K. L. Mackie, *J. Chem. Technol. Biotechnol.*, 2008, **34**, 101–110.
12 E. Palmqvist and B. Hahn-Hägerdal, *Bioresour. Technol.*, 2000, **74**, 25–33.
13 B. Alriksson, I. S. Horváth, A. Sjöde, N.-O. Nilvebrant and L. J. Jönsson, *Appl. Biochem. Biotechnol.*, 2005, **121–124**, 911–922.
14 B. Alriksson, A. Cavka and L. J. Jönsson, *Bioresour. Technol.*, 2011, **102**, 1254–1263.
15 L. J. Jönsson, E. Palmqvist, N.-O. Nilvebrant and B. Hahn-Hägerdal, *Appl. Microbiol. Biotechnol.*, 1998, **49**, 691–697.
16 M. Cantarella, L. Cantarella, A. Gallifuoco, A. Spera and F. Alfani, *Process Biochem.*, 2004, **39**, 1533–1542.
17 K. Zhang, M. Agrawal, J. Harper, R. Chen and W. J. Koros, *Ind. Eng. Chem. Res.*, 2011, **50**, 14055–14060.
18 S. Datta, Y. J. Lin, D. J. Schell, C. S. Millard, S. F. Ahmad, M. P. Henry, P. Gillenwater, A. T. Fracaro, A. Moradia, Z. P. Gwarnicki and S. W. Snyder, *Ind. Eng. Chem. Res.*, 2013, **52**, 13777–13784.
19 L. J. Jönsson, B. Alriksson and N.-O. Nilvebrant, *Biotechnol. Biofuels*, 2013, **6**, 16.
20 E. Palmqvist and B. Hahn-Hägerdal, *Bioresour. Technol.*, 2000, **74**, 17–24.
21 J. G. Wijmans and R. W. Baker, *J. Membr. Sci.*, 1995, **107**, 1–21.

22 L. M. Vane, *J. Chem. Technol. Biotechnol.*, 2005, **80**, 603–629.
23 F. Qin, S. Li, P. Qin, M. N. Karim and T. Tan, *Green Chem.*, 2014, **16**, 1262.
24 D. Cai, T. Zhang, J. Zheng, Z. Chang, Z. Wang, P. Qin and T. Tan, *Bioresour. Technol.*, 2013, **145**, 97–102.
25 F. Xiangli, Y. Chen, W. Jin and N. Xu, *Ind. Eng. Chem. Res.*, 2007, **46**, 2224–2230.
26 A. E. Ozcam, N. Petzetakis, S. Silverman, A. K. Jha and N. P. Balsara, *Macromolecules*, 2013, **46**, 9652–9658.
27 L. C. Basso, H. V. de Amorim, A. J. de Oliveira and M. L. Lopes, *FEMS Yeast Res.*, 2008, **8**, 1155–1163.
28 A. K. Jha, L. Chen, R. D. Offeman and N. P. Balsara, *J. Membr. Sci.*, 2011, **373**, 112–120.
29 A. Sluiter, B. Hames, R. Ruiz, C. Scarlata, J. Sluiter, D. Templeton and D. Crocker, *Determination of Structural Carbohydrates and Lignin in Biomass. Laboratory Analytical Procedure (LAP)*, Golden, CO, 2012.
30 V. D. Mitchell, C. M. Taylor and S. Bauer, *Bioenergy Res.*, 2014, **7**, 654–669.
31 J. Gmehling, U. Onken and J. R. Rarey-Nies, *Vapor-liquid equilibrium data collection*, Dechema, 1978.
32 *Perry's Chemical Engineers' Handbook*, ed. D. W. Green and R. H. Perry, McGraw-Hill Professional, 8th edn, 2007.
33 M. Sagehashi, T. Nomura, H. Shishido and A. Sakoda, *Bioresour. Technol.*, 2007, **98**, 2018–2026.
34 C. H. Lau, P. T. Nguyen, M. R. Hill, A. W. Thornton, K. Konstas, C. M. Doherty, R. J. Mulder, L. Bourgeois, A. C. Y. Liu, D. J. Sprouster, J. P. Sullivan, T. J. Bastow, A. J. Hill, D. L. Gin and R. D. Noble, *Angew. Chem., Int. Ed.*, 2014, **126**, 5426–5430.